ADVANCED MATERIALS
www.advmat.de

Universal Route to Impart Orthogonality to Polymer Semiconductors for Sub-Micrometer Tandem Electronics

Han Wool Park, Keun-Yeong Choi, Jihye Shin, Boseok Kang, Haejung Hwang, Shinyoung Choi, Aeran Song, Jaehee Kim, Hyukmin Kweon, Seunghan Kim, Kwun-Bum Chung, BongSoo Kim, Kilwon Cho, Soon-Ki Kwon, Yun-Hi Kim, Moon Sung Kang, Hojin Lee,* and Do Hwan Kim**

A universal method that enables utilization of conventional photolithography for processing a variety of polymer semiconductors is developed. The method relies on imparting chemical and physical orthogonality to a polymer film via formation of a semi-interpenetrating diphasic polymer network with a bridged polysilsesquioxane structure, which is termed an orthogonal polymer semiconductor gel. The synthesized gel films remain tolerant to various chemical and physical etching processes involved in photolithography, thereby facilitating fabrication of high-resolution patterns of polymer semiconductors. This method is utilized for fabricating tandem electronics, including pn-complementary inverter logic devices and pixelated polymer light-emitting diodes, which require deposition of multiple polymer semiconductors through solution processes. This novel and universal method is expected to significantly influence the development of advanced polymer electronics requiring sub-micrometer tandem structures.

Dissolution of polymer semiconductors in organic solvents provides unique opportunities for the fabrication of low-cost electronics by solution-based manufacturing processes.[1–3] This capability, however, serves as a double-edged sword during the fabrication of pixelated polymer heterostructures that are critical for manipulating charge carriers, excitons, and photons. This is because the underlying layer of the polymer film would be vulnerable to subsequent solution processing to which the successive layers are subjected for realization of the heterostructure, unless considerable care is taken to select solvents for the consecutive processes. This issue persists during not only the application of printing techniques[4–7] but also the processing of polymer semiconductors by photolithography, which is the workhorse in the present-day silicon industry. Utilization of photolithography for patterning polymer semiconductors would have a much stronger impact in the semiconductor industry than would that of any other presently available technology; this is because photolithography enables high-throughput patterning of polymer semiconductors at high resolution (<1 μm) by the use of facilities currently available in the industry.[8–10] However, generally,

H. W. Park, H. Hwang, J. Kim, H. Kweon, Prof. D. H. Kim
Department of Chemical Engineering
Hanyang University
Seoul 04763, Republic of Korea
E-mail: dhkim76@hanyang.ac.kr

K.-Y. Choi, Prof. H. Lee
School of Electronic Engineering
Soongsil University
Seoul 06978, Republic of Korea
E-mail: hojinl@ssu.ac.kr

J. Shin
Department of Chemical Engineering
Soongsil University
Seoul 06978, Republic of Korea

J. Shin, S. Kim, Prof. M. S. Kang
Department of Chemical and Biomolecular Engineering
Sogang University
Seoul 04107, Republic of Korea
E-mail: kangms@sogang.ac.kr

The ORCID identification number(s) for the author(s) of this article can be found under https://doi.org/10.1002/adma.201901400.

Dr. B. Kang, Prof. K. Cho
Department of Chemical Engineering
Pohang University of Science and Technology
Pohang 37673, Republic of Korea

S. Choi, Prof. B. Kim
Department of Chemistry
Ulsan National Institute of Science and Technology (UNIST)
Ulsan 44919, Republic of Korea

A. Song, Prof. K.-B. Chung
Division of Physics and Semiconductor Science
Dongguk University
Seoul 04620, Republic of Korea

Prof. S.-K. Kwon
Department of Materials Engineering and Convergence Technology
Gyeongsang National University
Jinju 52828, Republic of Korea

Prof. Y.-H. Kim
Department of Chemistry
Gyeongsang National University
Jinju 52828, Republic of Korea

DOI: 10.1002/adma.201901400

polymer semiconductor films are not chemically tolerant to common photoresists, developers, and strippers, as well as to organic solvents.[11,12] Moreover, such soft polymer films are typically not tolerant to the dry etching process, which is another critical step in fabricating well-pixelated polymer heterostructures at high resolution.[13–15] A promising attempt has been made to resolve this issue: development of a photoresist that does not affect the underlying polymer layer during the processing, which is termed an orthogonal photoresist.[16–21] Using a carefully designed orthogonal photoresist, the previous authors successfully patterned vacuum-deposited or solution-processed organic semiconductors with a minimal feature resolution of 2 μm.[22] However, despite this successful attempt, the use of such a photoresist-based methodology may not be the ultimate solution for realizing tandem electronics such as pn-junctions and pn-complementary logic devices through photolithography, since they require multiple semiconducting polymer layers. Sequential solution deposition and patterning of multiple polymer layers remain impossible tasks even with the use of orthogonal photoresists, because the underlying layer would be dissolved or swollen upon solution processing of the subsequent layer.

A more effective strategy is to impart orthogonality to the polymer semiconductors themselves, so that they can be subjected to a solution-based deposition process and photolithography as many times as required without deterioration of their intrinsic physical/optoelectronic properties. To this end, various methods have been developed for producing photo-crosslinked, physically crosslinked, and chemically crosslinked polymer semiconductors.[23–27] These methods rely on either anchoring crosslinkable moieties into the polymer side chains[23,24] or blending the polymers with crosslinkable organic additives.[25] However, the resulting polymer semiconductor films, which may be robust to subsequent chemical processes, remain vulnerable to the physical etching process, which causes difficulties in the assembling of high-resolution (sub-micrometer) tandem heterostructures via direct utilization of photolithography. Thus, alternative strategies that would facilitate taking full advantage of polymer semiconductors are highly sought after.

Here, we report, for the first time, a simple yet novel method for imparting both chemical and physical orthogonality to polymer semiconductor films, which will enable application of conventional photolithography, including sequential solution coating and physical etching processes, for fabrication of patterns at a sub-micrometer resolution. Importantly, this method is universally applicable to a wide range of polymer semiconductors that form semicrystalline or amorphous morphology in films. Tandem electronics requiring multiple layers of polymer semiconductors, such as pn-complementary inverter logic devices and pixelated polymer light-emitting diodes (PLEDs), were fabricated by the proposed method. Chemical and physical tolerance of the films was achieved via design of an orthogonal polymer semiconductor gel (OPSG) composed of a semi-interpenetrating diphasic polymer network (semi-IDPN) between the polymer semiconductors and bridged polysilsesquioxanes (BPSQs). The introduction of the BPSQ framework did not deteriorate the essential optoelectronic properties of the polymer semiconductors. Our novel and universal method can contribute toward practical realization of high-resolution polymer optoelectronics.

Figure 1a shows a schematic of the OPSG fabricated by converting a sol containing a mixture of a polymer semiconductor and an organosilica precursor into a semi-IDPN through an interactive sol–gel process.[28–35] Figure 1b shows the chemical structure of the representative organosilica precursor [bis(trichlorosilyl)alkane (BTS-C*n*) and bis(trichlorosilylethyl) benzene (BTS-Ph)] used in this work. The chlorine species in the precursor molecules are substituted with hydroxides in the presence of a marginal amount of moisture and, thereby, silanols are formed. Upon annealing, the silanols in the neighboring molecules undergo a condensation reaction to form a ladder-like network of the BPSQs with molecular pores (Figure S1, Supporting Information). Thermal condensation to siloxane groups in a ladder-like structure (with Si–O–Si stretching vibrations near 1086 and 1023 cm^{-1}) (Figures S2 and S3, Supporting Information) was confirmed by Fourier transform infrared (FT-IR) spectroscopy (Figure 1c).[36–38] The resulting BPSQ framework was uniformly distributed over the entire OPSG film without apparent macroscopic phase separation; the signal distribution of the elements (S^- and SiC^-) as determined by time-of-flight secondary ion mass spectrometry (ToF-SIMS) analysis upon etching was uniform over the entire thickness of the film (Figure 1d; Figures S4–S6, Supporting Information).[39,40] We conjecture that the less-ordered phase of the BPSQ framework enabled the semiconducting polymer chains to effectively interpenetrate into the BPSQs, resulting in the formation of well-defined OPSG films.[41] The resulting OPSG films exhibited chemical and physical tolerance to external stimuli, which was not the case with the pristine polymer films. No changes were observed with the naked eye when various OPSG films (made of poly[2,5-bis(2-decyl-dodecyl)pyrrolo[3,4-*c*]pyrrole-1,4(2*H*,5*H*)-dione-(*E*)- 1,2-di(2,2′-bithiophen-5-yl)ethene] (PDPP-TVT),[42] poly(3-hexylthiophene) (P3HT), poly[4,8-bis(5-(2-ethylhexyl)thiophen-2-yl)-benzo[1,2-*b*;4,5-*b*′]dithiophene-2,6-diyl-*alt*-(4-(2-ethylhexyl)-3-fluorothieno[3,4-*b*]thiophene-)-2-carboxylate-2-6-diyl)] (PTB7-Th),[43] poly[2,5-(2-octyldodecyl)-3,6-diketopyrrolopyrrole-*alt*-5,5-(2,5-di(thien-2-yl)thieno [3,2-*b*]thiophene)] (PDPP-DTT), and poly[(*E*)-2,7-bis(2-decyl tetradecyl-4-(5-methylthiophen-2-yl)-9-(5′-(2-(5-methylthiophen-2-yl)vinyl)-[2,2′-bithiophen]-5-yl)-benzo[*lmn*][3,8] phenanthroline-1,3,6,8(2*H*,7*H*)-tetraone (PNDI-BTE)[44] were dipped into and removed from a chemical bath of chlorobenzene (C_6H_5Cl) or chloroform ($CHCl_3$), both of which are good solvents for the tested polymers (Figure 1e; Movies S1–S4, Supporting Information). The chemical tolerance of the OPSG films fabricated by using various types of BTS-C*n* (-C3, -C6, -C8, and -C10) and BTS-Ph precursors was further confirmed by the negligible change in film thickness after the chemical treatment with C_6H_5Cl and $CHCl_3$ (Figure S7, Supporting Information). The OPSG films also exhibited strong resistance to abrasion; the OPSG films, unlike their pristine counterparts, could not be easily removed by swiping with a cotton swab (Figure 1e; Figure S8 and Movie S5, Supporting Information). Even though the OPSG films and the corresponding pristine polymer films did not show any noticeable difference in the plane-view morphology obtained by atomic force microscopy (AFM) (Figures S9–S13, Supporting

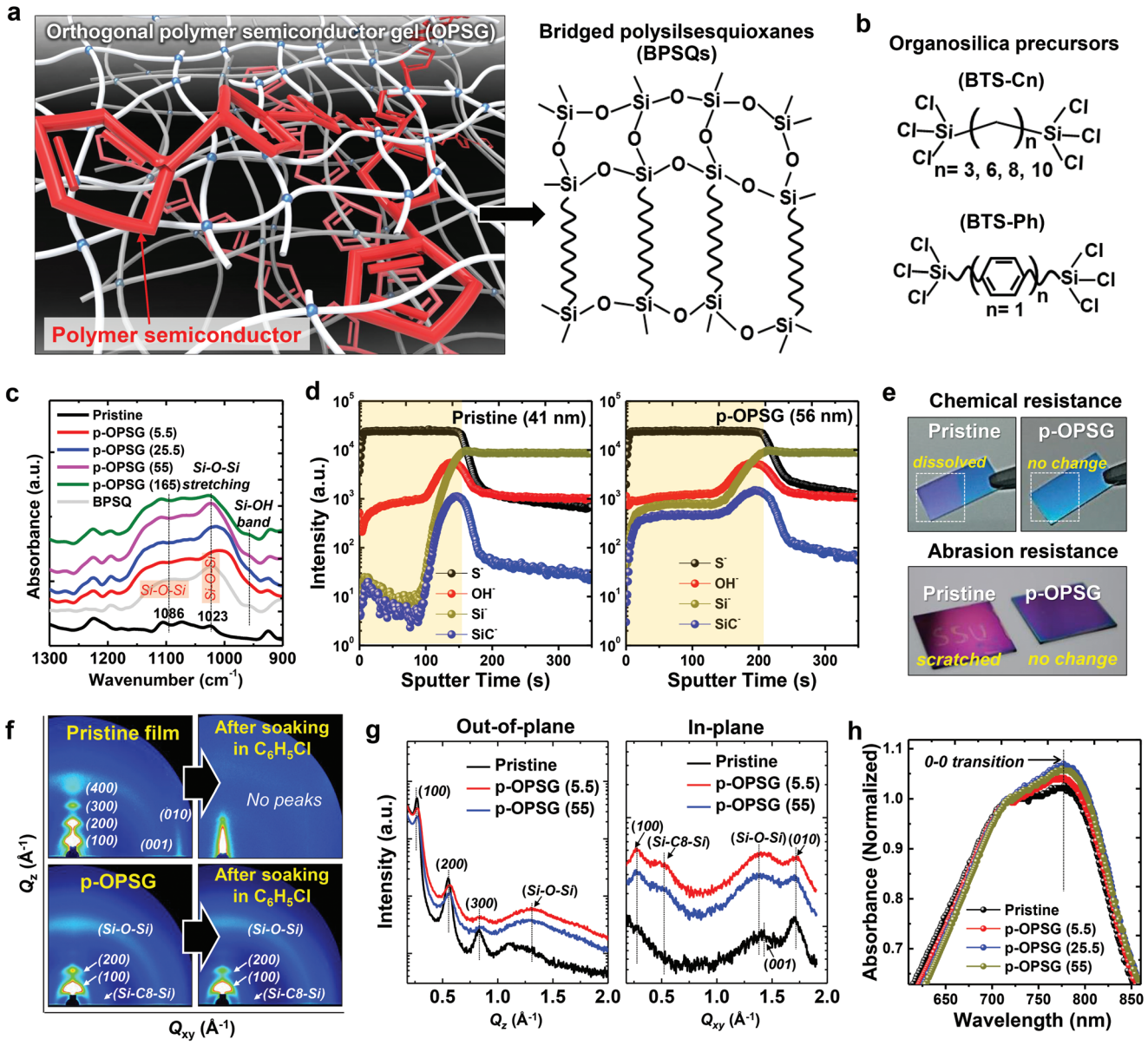

Figure 1. Design and characterization of OPSG films with semi-IDPN. a) Schematic description of OPSG composed of polymer semiconductor interpenetrated into BPSQ network. b) Chemical structures of organosilica precursors (BTS-C*n* and BTS-Ph). c) FT-IR spectra of PDPP-TVT-based OPSG films fabricated using different concentrations (wt%) of BTS-C8 precursor. The blend solution is prepared by dissolving the semiconducting polymers and organosilica precursors with designed weight ratio in C_6H_5Cl. d) ToF-SIMS profiles of pristine PDPP-TVT film and OPSG film. e) Photographs of PDPP-TVT-based OPSG film showing resistance to chemical treatment (top) and abrasion (bottom). f) Synchrotron 2D-GIXD patterns of pristine PDPP-TVT film and PDPP-TVT-based OPSG film before and after soaking in C_6H_5Cl. g) 1D analysis of diffraction patterns of PDPP-TVT-based OPSG films. h) UV–vis–NIR spectra of PDPP-TVT-based OPSG films fabricated using different concentrations (wt%) of BTS-C8 precursor.

Information), introduction of the BPSQs resulted in changes in the microstructure of the polymer films. Figure 1f,g, respectively, shows the 2D grazing incidence X-ray diffraction (2D-GIXD) patterns and results of the corresponding 1D analysis in the out-of-plane and in-plane directions for a PDPP-TVT-based OPSG film. These results show that the crystallinity of the OPSG film is suppressed compared to that of the pristine film. Additionally, two ring-like features were observed in the diffraction pattern of the OPSG films, which can be assigned to peaks derived from the BPSQ template, which has a ladder-like structure (Figure S14, Supporting Information); the peaks located at 0.513 and 1.414 $Å^{-1}$ correspond to the width (defined by Si–C8–Si) and thickness (defined by Si–O–Si), respectively, of the ladder structure. The suppressed crystallinity of the polymer semiconductors in the OPSG film is attributed to the limited motion of the polymer chain confined in the BPSQ network, which prevents formation of crystalline domains over a long range.[41] This suppression of crystallinity was also observed for the OPSGs based on other polymer semiconductors such as PNDI-BTE and P3HT (Figures S15 and S16, Supporting

Information). Furthermore, the 2D-GIXD pattern did not show any noticeable change when the film was chemically treated with C_6H_5Cl (Figure 1f; Figure S17, Supporting Information). While the long-range order, i.e., crystallinity, of the polymers in the OPSGs had weakened compared to that in the pristine film, the extent of the aggregation formation in films remained comparable or even improved, which has recently been demonstrated to play more vital role in determining the electrical transport properties of the polymer semiconductor films.[45,46] UV–vis–NIR spectra of p-type PDPP-TVT-based OPSG films were measured for different concentrations of the BTS-C8 precursor (Figure 1h; Figure S18, Supporting Information). The OPSGs yielded a stronger absorbance associated with the 0–0 transition, reflecting that the formation of aggregates is amplified in the presence of BPSQ network.

The electrical characteristics of the OPSG films were examined using a field-effect transistor (FET) test bed in a bottom-gate, top-contact geometry. The influence of the BPSQ network in the OPSGs could be studied by carefully examining the device characteristics following the sol–gel reaction promoted by thermal annealing. **Figure 2**a shows the transfer curves of a p-type PDPP-TVT-based OPSG FET that were obtained before (blue) and after (red) thermal annealing (at 180 °C for 3 h). Before annealing of the OPSGs, the FET was hardly modulated by the gate, which is typical behavior for a transistor with a degenerately doped channel. We attribute the doping to the presence of chlorine species in the bulk of the OPSG film that are released from the employed organosilica precursors[31,47] (Figure S19, Supporting Information). Another doping source could be the silanol groups present in the OPSG bulk that can trap electrons to become negatively charged species ($-Si-O^-$).[48] Upon annealing the film, the silanol groups could undergo a water condensation reaction (Figure 2b,c), and, therefore, FETs with well-resolved gate modulation could be obtained. Series of transfer characteristics for FETs based on pristine PDPP-DTT films and the corresponding OPSG films that are annealed at different conditions are shown in Figures S20–S23 and Movie S2 in the Supporting Information.

Figure 2d shows the transfer curves of FETs based on annealed OPSGs made of p-type PDPP-TVT, PDPP-DTT, PTB7-Th, PCDTPT, and n-type PNDI-BTE. The mobility (extracted at $V_{DS} = -40$ V or 40 V) of the p- or n-type OPSG FETs (red) based on various polymer semiconductors was found to be comparable or even superior to that of the pristine film FETs (black) (Figure 2e; Table S3, Supporting Information). The slight increase in mobility could be attributed to the enhanced extent of aggregation formation for the polymer chains confined in the BPSQ network. Further, to investigate the environmental stability of the p- or n-type OPSG FETs, the transfer characteristics of the pristine PDPP-DTT or PNDI-BTE FETs and the corresponding p- or n-type OPSG FETs were collected over a period of time, which displays that the rate of degradation between the pristine FETs and OPSG FETs was comparable, indicating that residual, uncondensed chlorine species do not make a significant influence on environmental stability for OPSG FETs (Figures S24 and S25, Supporting Information). PDPP-DTT-based OPSG FETs also yielded stronger tolerance to bias-stress compared to those made with pritine PDPP-DTT film (Figure S26, Supporting Information), suggesting that a smaller number of traps is present in the OPSG films.

The chemical robustness of the electrical performance of the FETs based on the OPSG films was examined by comparing the transfer characteristics before and after soaking of the FETs into a chemical bath of C_6H_5Cl. Figure 2f shows a series of transfer curves for the p-type PDPP-TVT-based OPSG FETs and n-type PNDI-BTE-based OPSG FETs that were obtained after their chemical treatment with C_6H_5Cl, which was the original solvent used to prepare the PDPP-TVT and PNDI-BTE films. The results reveal the highly orthogonal nature of the device to the subsequent chemical processes after formation of the gel network. Such a chemical robustness of the electrical performance was consistently observed for the OPSG FETs based on semicrystalline P3HT, PDPP-DTT, and PTB7-Th as well as those based on fully amorphous poly(bis(4-phenyl) (2,4,6-trimethylphenyl)amine) (PTAA) (Figures S27 and S28, Supporting Information). The results indicate that the approach is even applicable to impart orthogonality to amorphous polymers. Very importantly, the reliable device operation following the chemical treatment indicates that the OPSG FETs can be operated even after being subjected to sequential solution processes that are necessary for fabricating tandem electronics. We again emphasize that sequential solution coating of polymer semiconductors is, in general, highly challenging since the underlying layer would be easily dissolved or swollen during the deposition of subsequent layers.

Another novel feature of the fabricated OPSG films with the semi-IDPN is that they show significant tolerance to the physical etching process—which is a key step for transferring the high-resolution patterns of the photoresist onto the underlying materials—without significant damage. **Figure 3**a shows detailed AFM images of sub-micrometer patterns obtained from a p-type PDPP-TVT-based OPSG film and an n-type PNDI-BTE-based OPSG film with a feature size as small as 800–950 nm, which also exhibited high tolerance to chemical treatment with C_6H_5Cl (Figure S29, Supporting Information). The OPSG films not only exhibited strong chemical tolerance to photoresists, developers, and strippers but also showed high physical tolerance to the reactive ion etching (RIE) process used for patterning the layer, without significant damage from side-etching (Figure 3b). In contrast, the pristine films did not exhibit the desired chemical/physical tolerance during the photolithography processes; only a fraction of the polymer films survived the photolithography processes, and these survived patterns exhibited noticeable side-etching (Figure 3a,b). The difference in the etching rate between the OPSG films and their pristine counterparts—which was estimated from the thickness variation following etching of the films under the same RIE condition—further supports our belief that the introduction of the semi-IDPN imparts physical orthogonality to etching processes (Figure 3c). Furthermore, well-defined micropatterns with various sizes and shapes could be reliably prepared from OPSG films over a large area through conventional photolithography, which involves multiple chemical and etching processes (Figure 3d; Figure S30, Supporting Information). In particular, the demonstrated physical tolerance to etching processes opens new avenues for performing sub-micrometer patterning with precise control of the shape and height profile. We emphasize

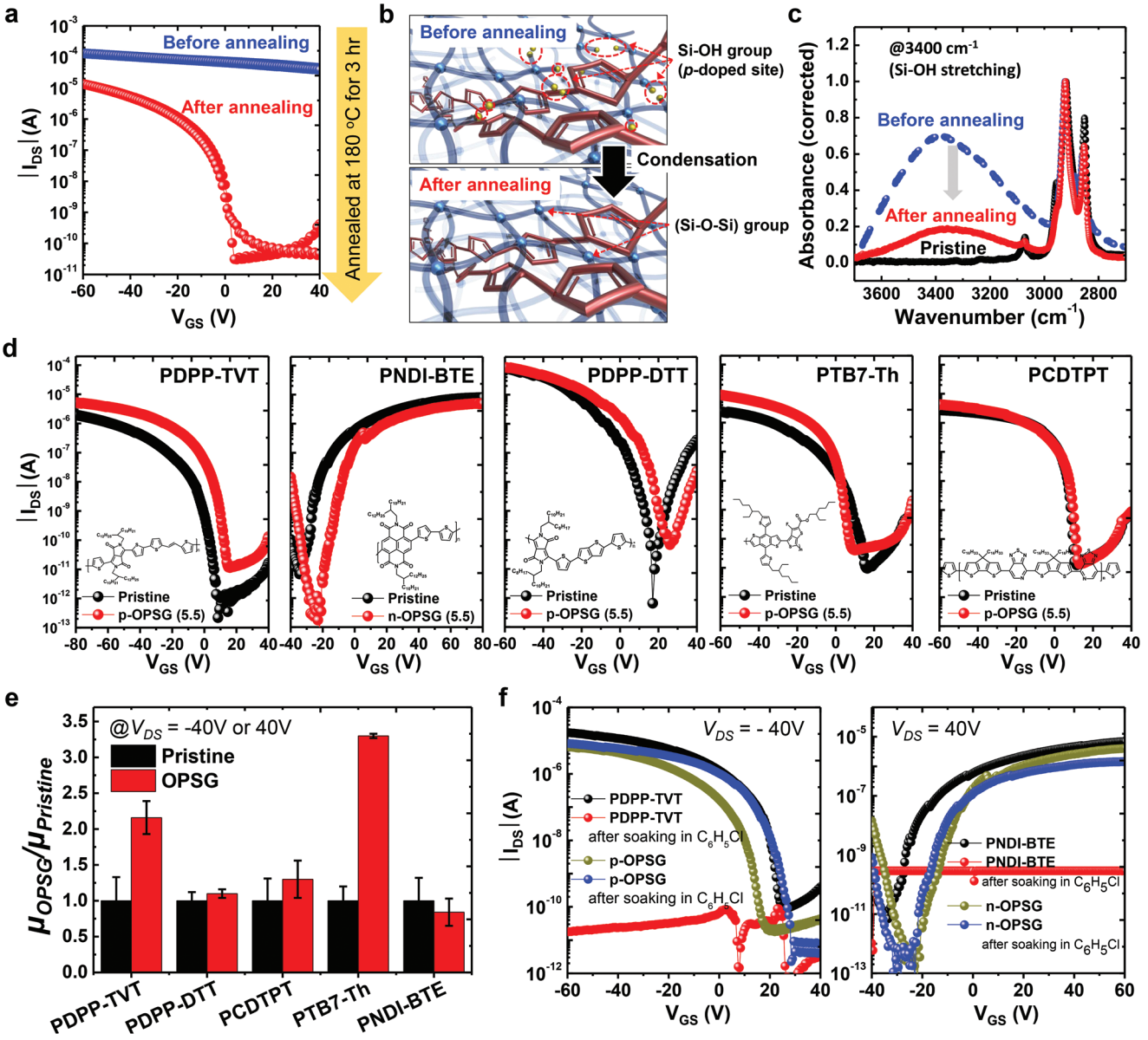

Figure 2. Electrical characteristics of OPSGs. a) Transfer characteristics of p-type PDPP-TVT-based OPSG FETs before (blue) and after (red) thermal annealing (at 180 °C for 3 h). b) Schematic of change in molecular structure of OPSG film upon annealing. c) FT-IR spectra (in the wavenumber range showing Si–OH stretching near 3400 cm^{-1}) of pristine PDPP-TVT film (black) and corresponding OPSG film before (blue) and after (red) thermal annealing. d) Comparison of transfer characteristics of various polymer semiconductors in OPSGs (red) and their pristine (black) forms (p-type PDPP-TVT, PDPP-DTT, PTB7-Th, PCPTBT, and n-type PNDI-BTE) (wt%). The blend solution is prepared by dissolving the semiconducting polymers and organosilica precursors with designed weight ratio in C_6H_5Cl. e) Summary of field effect mobilities of OPSGs based on various polymer semiconductors normalized with mobilities of corresponding pristine polymer films. f) Series of transfer characteristics of p- and n-type FETs before and after soaking in C_6H_5Cl.

that realization of sub-micrometer patterns of polymer semiconductors by an approach based on orthogonal photoresists would be difficult. This is because the delicate organic layers are prone to side-etching, especially when the pattern resolution becomes lower than the micrometer-scale resolution.

As a proof of concept, for exploitation of the chemical/physical orthogonality of the OPSGs, two different applications that require tandem processing of polymer semiconductor layers are demonstrated. First, a basic complementary metal–oxide–semiconductor (CMOS) inverter was fabricated, which requires patterning of p- and n-type polymer channels in sequence (**Figure 4**a; see Figure S31 in the Supporting Information for the detailed fabrication process). Figure 4a shows an optical microscopy image of fabricated inverter circuits having 5 μm complementary channels prepared by subjecting an n-type PNDI-BTE-based OPSG channel over a p-type PDPP-TVT-based OPSG channel to a series of solution processes. Figure 4b shows the transfer curves of the p-channel that were

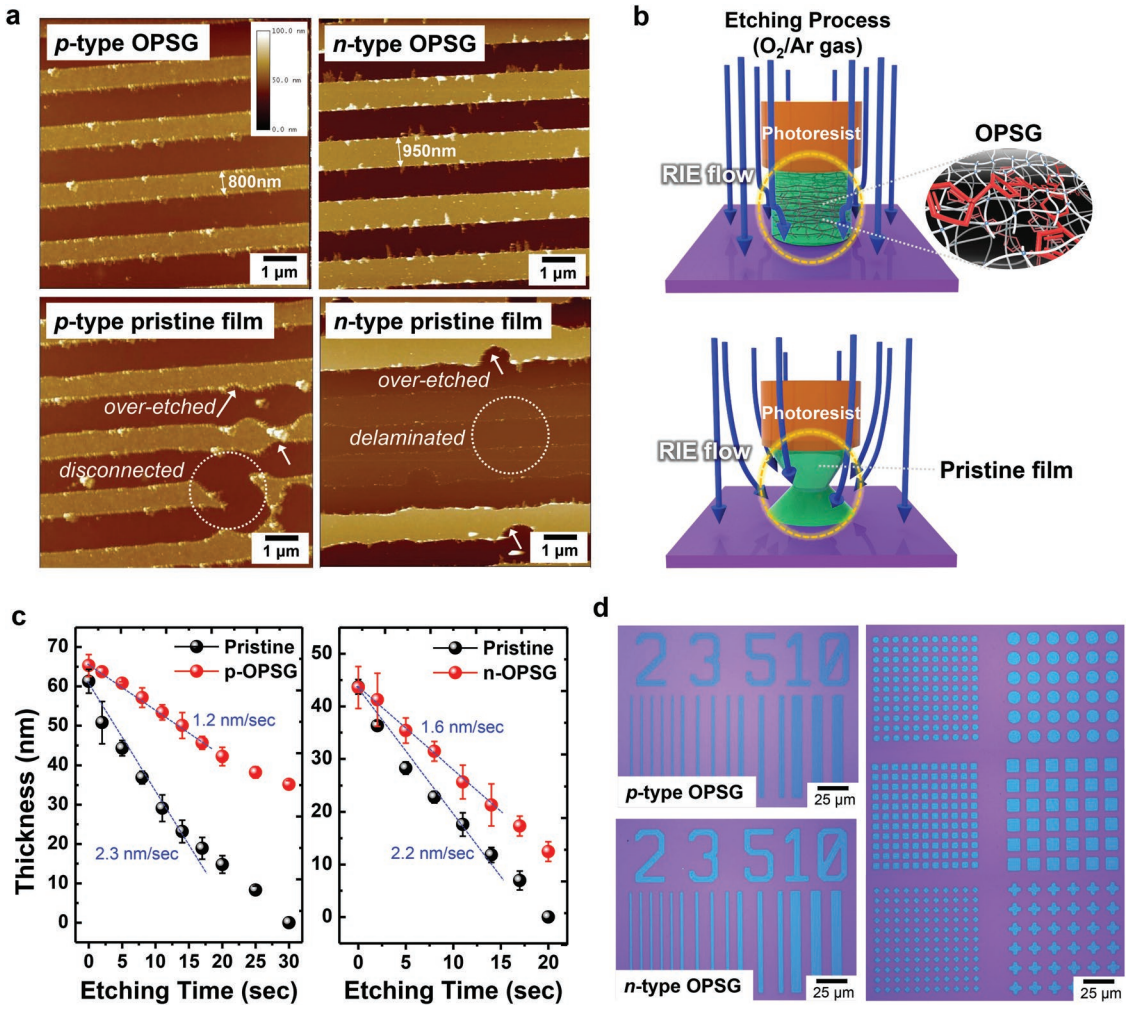

Figure 3. High-resolution patterns prepared from OPSG films by conventional photolithography. a) AFM images of sub-micrometer patterns derived from p-type PDPP-TVT-based OPSG film and n-type PNDI-BTE-based OPSG film. Those derived from pristine polymer films are also shown for comparison. b) Schematic of different etching behavior for pristine and OPSG films. c) Etching characteristics of p- and n-type OPSG films determined from thickness variation following etching of films. d) Optical microscopy images of well-defined micropatterns with various sizes and shapes prepared from OPSG films by conventional photolithography.

obtained before (black line: pristine film; blue line: OPSG film) and after (red line: pristine film; dark yellow line: OPSG film) patterning of the n-channel on the side. Even though the photolithography process was required for preparation of the n-channel, the underlying p-channel did not show noticeable degradation in its performance. In contrast, when the p-channel was fabricated using the pristine PDPP-TVT layer, the film was removed during the subsequent process performed to form the n-channel; thus, the electrical characteristics of the p-channel could not be examined. Figure 4c shows the DC voltage transfer and voltage gain curves of CMOS inverter prepared using the as-prepared p-type OPSG channel ($W/L = 50/5$ μm) and as-prepared n-type OPSG channel ($W/L = 100/5$ μm). When the input voltage was swept from 0 to 100 V at a supply voltage (V_{DD}) of 60 V, a voltage inversion in the output signal occurred at 58.5 V, with a voltage gain of 8. Figure 4d shows the transient response of the CMOS inverter with an input pulse of 60 Hz, which confirms that the input pulses were successfully reproduced as the inverted output signals without any time delay or voltage loss. As the frequency increased, the p-type OPSG-based inverter could still maintain its transient characteristics up to 2 kHz, though its frequency responses began to be distorted by the resistance–capacitance (RC) delay afterward (Figure S32, Supporting Information).

We also fabricated micropatterned two-color (red and green) pixels by tandem processing of OPSGs with two different light-emitting polymers placed side by side: poly[2-methoxy-5-(2′-ethylhexyloxy)-*p*-phenylene vinylene] (MEH-PPV, red) and poly(9,9-dioctylfluorene-*co*-bithiophene) (F8T2, green). Figure 4e shows a fluorescence microscopy image of patterned pixels (20 μm × 20 μm) of MEH-PPV- and F8T2-based OPSGs that were fabricated by photolithography. Well-resolved pixels with distinct colors (red and green, respectively) can be seen. Patterning of MEH-PPV and F8T2 in their pristine form was indeed possible via selection of an appropriate combination of orthogonal solvents (Figure S33, Supporting Information). However, the underlying pixels of pristine F8T2 were stained after processing of the top MEH-PPV layer, resulting

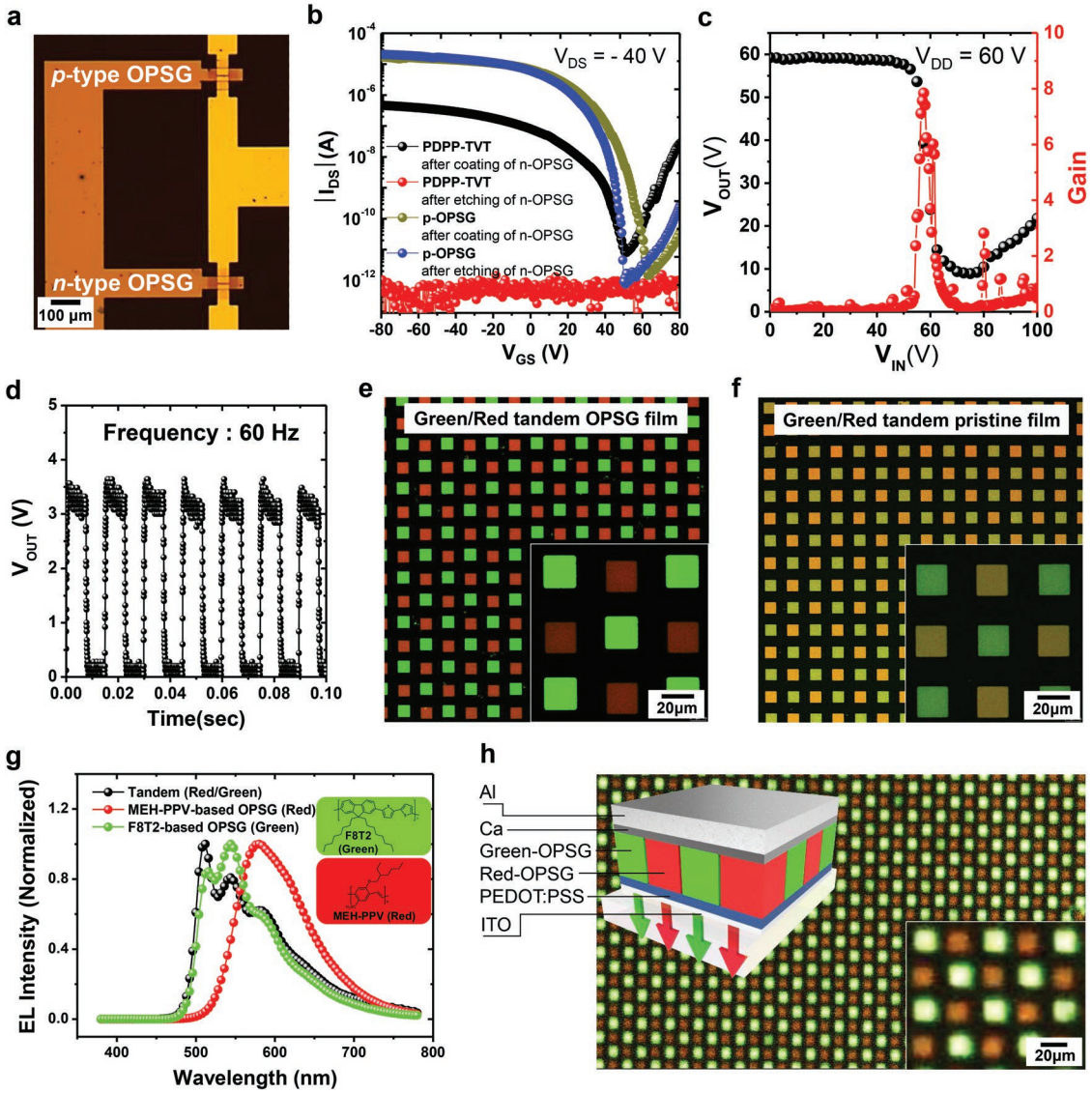

Figure 4. High-resolution tandem devices based on OPSG films. a) Optical microscopy image of CMOS inverter circuit having 5 μm complementary channels fabricated by a series of solution processes and photolithography. The PNDI-BTE-based OPSG was used as the n-channel and the PDPP-TVT-based OPSG was used as the p-channel. b) Transfer characteristics of p-channel measured before and after patterning of n-channel. c) DC voltage transfer characteristics and voltage gain of CMOS inverter at V_{DD} = 60 V. d) Transient response of CMOS inverter with input pulse of 60 Hz. e,f) Fluorescence microscopy images of patterned pixels (red and green) of light-emitting polymer gel and pristine films fabricated by sequential solution coating and photolithography. g) EL spectrum of pixelated PLED fabricated by tandem processes, showing two distinct peaks at 544 and 580 nm corresponding to EL from F8T2 and MEH-PPV, respectively. Inset shows chemical structures of two light-emitting polymers. h) Optical microscopy image of pixelated PLED. Inset shows a schematic structure of PLED device fabricated in this work.

in color change from red to orange (Figure 4f). We also fabricated PLEDs with micropatterns of MEH-PPV- and F8T2-based OPSGs (see the Supporting Information for the detailed fabrication process). These PLEDs yielded device performances comparable to the pristine polymer-based PLEDs we made and to those reported for the state-of-the-art devices (Figures S34 and S35 and Tables S4 and S5, Supporting Information) The electroluminescence (EL) spectrum (black) of the device matched with the combination of the EL spectra obtained from F8T2 (green) and MEH-PPV (red), separately (Figure 4g). Both the spectrum and the optical microscopy image (Figure 4h) of the pixelated PLED device under operation indicate that the OPSGs based on light-emitting polymers can also be fabricated by photolithography and etching without significant degradation of the optical performances (Movie S6, Supporting Information). Moreover, the exceptional orthogonality of the light-emitting polymer gels would enable the fabrication of PLED devices that exhibit separate red, green, and blue spectra, which will probably have a significant impact on the development of high-resolution OLED displays.

A method for conversion of a layer of solution-processed polymer semiconductors into a layer chemically and physically tolerant to subsequent solution and etching processes can provide unprecedented opportunities in the field of polymer

electronics. Such a method would enable direct application of conventional photolithography to the large-scale fabrication of high-resolution patterns of polymer semiconductors. In this study, we demonstrated that the above-described conversion could be achieved simply by introducing a BPSQ network into various polymer semiconductors. In addition to acquiring chemical orthogonality, the resulting OPSGs with a semi-IDPN structure also acquired physical orthogonality to etching processes, and the resulting electronic properties of the material were not degraded. Consequently, both the sub-micrometer patterning of polymer semiconductors and the tandem fabrication of polymer devices such as pn-complementary inverters and pixelated two-color (red and green) PLEDs could be realized by conventional photolithography. Ultimately, the proposed strategy is expected to open up new avenues for the fabrication of optoelectronic devices that require high-resolution tandem processing of polymer semiconductors such as OLED microdisplays, organic CMOS image sensors, and artificial eyes.

Experimental Section

Detailed experimental processes are provided in the Supporting Information.

Supporting Information

Supporting Information is available from the Wiley Online Library or from the author.

Acknowledgements

H.W.P. and K.-Y.C. contributed equally to this work. This work was supported by the Samsung Research Funding & Incubation Center of Samsung Electronics under Project Number SRFC-MA1501-04.

Conflict of Interest

The authors declare no conflict of interest.

Keywords

orthogonal polymer semiconductor gel, photolithography, semi-interpenetrating diphasic polymer network, sequential solution processes, sub-micrometer tandem electronics

Received: March 3, 2019
Revised: April 5, 2019
Published online: May 7, 2019

[1] G. Li, W.-H. Chang, Y. Yang, *Nat. Rev. Mater.* **2017**, *2*, 17043.
[2] J. A. Rogers, T. Someya, Y. Huang, *Science* **2010**, *327*, 1603.
[3] A. C. Arias, J. D. MacKenzie, I. McCulloch, J. Rivnay, A. Salleo, *Chem. Rev.* **2010**, *110*, 3.
[4] J. Ha, S. Chung, M. Pei, K. Cho, H. Yang, Y. Hong, *ACS Appl. Mater. Interfaces* **2017**, *9*, 8819.
[5] F. Ge, X. Wang, Y. Zhang, E. Song, G. Zhang, H. Lu, K. Cho, L. Qiu, *Adv. Electron. Mater.* **2017**, *3*, 1600402.
[6] B. A. Ridley, B. Nivi, J. M. Jacobson, *Science* **1999**, *286*, 746.
[7] S. R. Forrest, *Nature* **2004**, *428*, 911.
[8] H. S. Hwang, A. A. Zakhidov, J.-K. Lee, X. André, J. A. DeFranco, H. H. Fong, A. B. Holmes, G. G. Malliaras, C. K. Ober, *J. Mater. Chem.* **2008**, *18*, 3087.
[9] S. J. Lee, Y.-J. Kim, S. Y. Yeo, E. Lee, H. S. Lim, M. Kim, Y.-W. Song, J. Cho, J. A. Lim, *Sci. Rep.* **2015**, *5*, 14010.
[10] S. De Vusser, S. Steudel, K. Myny, J. Genoe, P. Heremans, *Appl. Phys. Lett.* **2006**, *88*, 103501.
[11] J. A. DeFranco, B. S. Schmidt, M. Lipson, G. G. Malliaras, *Org. Electron.* **2006**, *7*, 22.
[12] I. Kymissis, C. D. Dimitrakopoulos, S. Purushothaman, *J. Vac. Sci. Technol., B: Microelectron. Nanometer Struct.* **2002**, *20*, 956.
[13] A. P. Quist, E. Pavlovic, S. Oscarsson, *Anal. Bioanal. Chem.* **2005**, *381*, 591.
[14] A. A. Zakhidov, J.-K. Lee, H. H. Fong, J. A. DeFranco, M. Chatzichristidi, P. G. Taylor, C. K. Ober, G. G. Malliaras, *Adv. Mater.* **2008**, *20*, 3481.
[15] L. Zhang, H. Liu, Y. Zhao, X. Sun, Y. Wen, Y. Guo, X. Gao, C.-a Di, G. Yu, Y. Liu, *Adv. Mater.* **2012**, *24*, 436.
[16] P. G. Taylor, J.-K. Lee, A. A. Zakhidov, M. Chatzichristidi, H. H. Fong, J. A. DeFranco, G. G. Malliaras, C. K. Ober, *Adv. Mater.* **2009**, *21*, 2314.
[17] J.-K. Lee, P. G. Taylor, A. A. Zakhidov, H. H. Fong, H. S. Hwang, M. Chatzichristidi, G. G. Malliaras, C. K. Ober, *J. Photopolym. Sci. Technol.* **2009**, *22*, 565.
[18] J. Jang, Y. Song, H. Oh, D. Yoo, D. Kim, H. Lee, S. Hong, J.-K. Lee, T. Lee, *Appl. Phys. Lett.* **2014**, *104*, 24_1.
[19] A. A. Zakhidov, J.-K. Lee, J. A. DeFranco, H. H. Fong, P. G. Taylor, M. Chatzichristidi, C. K. Ober, G. G. Malliaras, *Chem. Sci.* **2011**, *2*, 1178.
[20] J.-K. Lee, H. H. Fong, A. A. Zakhidov, G. E. McCluskey, P. G. Taylor, M. Santiago-Berrios, H. D. Abruna, A. B. Holmes, G. G. Malliaras, C. K. Ober, *Macromolecules* **2010**, *43*, 1195.
[21] D. Lyashenko, A. Perez, A. Zakhidov, *Phys. Status Solidi A* **2017**, *214*, 1600302.
[22] J. F. Chang, M. C. Gwinner, M. Caironi, T. Sakanoue, H. Sirringhaus, *Adv. Funct. Mater.* **2010**, *20*, 2825.
[23] E. K. Lee, C. H. Park, J. Lee, H. R. Lee, C. Yang, J. H. Oh, *Adv. Mater.* **2017**, *29*, 1605282.
[24] L. Qiu, Q. Xu, W. H. Lee, X. Wang, B. Kang, G. Lv, K. Cho, *J. Mater. Chem.* **2011**, *21*, 15637.
[25] R.-Q. Png, P.-J. Chia, J.-C. Tang, B. Liu, S. Sivaramakrishnan, M. Zhou, S.-H. Khong, H. S. Chan, J. H. Burroughes, L.-L. Chua, *Nat. Mater.* **2010**, *9*, 152.
[26] C.-Y. Nam, Y. Qin, Y. S. Park, H. Hlaing, X. Lu, B. M. Ocko, C. T. Black, R. B. Grubbs, *Macromolecules* **2012**, *45*, 2338.
[27] H. J. Kim, A.-R. Han, C.-H. Cho, H. Kang, H.-H. Cho, M. Y. Lee, J. M. Fréchet, J. H. Oh, B. J. Kim, *Chem. Mater.* **2012**, *24*, 215.
[28] J. Livage, *Curr. Opin. Solid State Mater. Sci.* **1997**, *2*, 132.
[29] A. Celzard, J. Mareche, *J. Chem. Educ.* **2002**, *79*, 854.
[30] R. Vendamme, S.-Y. Onoue, A. Nakao, T. Kunitake, *Nat. Mater.* **2006**, *5*, 494.
[31] M.-H. Yoon, H. Yan, A. Facchetti, T. J. Marks, *J. Am. Chem. Soc.* **2005**, *127*, 10388.
[32] Y.-Y. Noh, H. Sirringhaus, *Org. Electron.* **2009**, *10*, 174.
[33] S. Jung, M. Albariqi, G. Gruntz, T. Al-Hathal, A. Peinado, E. Garica-Caurel, Y. Nicolas, T. Toupance, Y. Bonnassieux, G. Horowitz, *ACS Appl. Mater. Interfaces* **2016**, *8*, 14701.
[34] S. Altmann, J. Pfeiffer, *Monatsh. Chem.* **2003**, *134*, 1081.
[35] H. Jiang, Z. Zheng, Z. Li, X. Wang, *Ind. Eng. Chem. Res.* **2006**, *45*, 8617.

[36] H. Seki, T. Kajiwara, Y. Abe, T. Gunji, *J. Organomet. Chem.* **2010**, *695*, 1363.
[37] S. S. Choi, A. S. Lee, H. S. Lee, H. Y. Jeon, K. Y. Baek, D. H. Choi, S. S. Hwang, *J. Polym. Sci., Part A: Polym. Chem.* **2011**, *49*, 5012.
[38] E. Park, H. Ro, C. Nguyen, R. Jaffe, D. Yoon, *Chem. Mater.* **2008**, *20*, 1548.
[39] L. A. Utracki, C. A. Wilkie, *Polymer Blends Handbook*, Springer, Dordrecht, The Netherlands **2002**.
[40] R. Paul, U. Karabiyik, M. C. Swift, A. R. Esker, *Langmuir* **2008**, *24*, 5079.
[41] K. Yu, B. Park, G. Kim, C.-H. Kim, S. Park, J. Kim, S. Jung, S. Jeong, S. Kwon, H. Kang, *Proc. Natl. Acad. Sci. USA* **2016**, *113*, 14261.
[42] I. Kang, T. K. An, J.-a Hong, H. J. Yun, R. Kim, D. S. Chung, C. E. Park, Y. H. Kim, S. K. Kwon, *Adv. Mater.* **2013**, *25*, 524.
[43] S. H. Liao, H. J. Jhuo, Y. S. Cheng, S. A. Chen, *Adv. Mater.* **2013**, *25*, 4766.
[44] R. Kim, P. S. Amegadze, I. Kang, H. J. Yun, Y. Y. Noh, S. K. Kwon, Y. H. Kim, *Adv. Funct. Mater.* **2013**, *23*, 5719.
[45] R. Noriega, J. Rivnay, K. Vandewal, F. P. Koch, N. Stingelin, P. Smith, M. F. Toney, A. Salleo, *Nat. Mater.* **2013**, *12*, 1038.
[46] S. Wang, S. Fabiano, S. Himmelberger, S. Puzinas, X. Crispin, A. Salleo, M. Berggren, *Proc. Natl. Acad. Sci. USA* **2015**, *112*, 10599.
[47] C. Kim, Z. Wang, H.-J. Choi, Y.-G. Ha, A. Facchetti, T. J. Marks, *J. Am. Chem. Soc.* **2008**, *130*, 6867.
[48] S. Jeong, D. Kim, B. K. Park, S. Lee, J. Moon, *Nanotechnology* **2007**, *18*, 025204.